

Supplemental Materials

Molecular Biology of the Cell

Yang et al.

Supplementary Figure 1

PKC inhibitors, bisindolylmaleimide-1 and GO6976 prevented PDBu-induced changes in growth cone morphology and actin network distribution.

(A) DIC images of a growth cone under control conditions, 10 min after treatment with PDBu (100 nM), and 20 min after wash-in bisindolylmaleimide-1 (BIS, 10 μ M) in continued presence of PDBu. Dashed lines note the C-domain boundary. BIS wash-in reversed the PDBu induced contractile response in the C-domain.

(B) Phalloidin labeling of growth cones to compare the effect of PDBu treatment under control, GO or BIS backgrounds (10 μ M, 10 min pretreatment). Both GO and BIS prevented the changes in actin network distribution associated with PDBu. Scale bars 10 μ m.

Supplementary Figure 2

PKC reorganized actin networks independent of microtubule dynamics.

Growth cones were treated with DMSO (control), PDBu (100 nM, 10 min), taxol (1 μ M, 30 min), or pretreated with taxol (30 min) followed by co-treatment with taxol and PDBu for 10 min, fixed and labeled with phalloidin (left and red channel) and microtubule antibody (middle column and green channel). P: peripheral domain; T: transition zone; C: central domain; red arrowhead: filopodium; asterisk: actin veil; yellow open arrowhead: actin arcs; yellow arrow: intrapodia; red dotted circle: contractile node; yellow dotted line traces the leading edge; orange dotted line marks the proximal P-domain boundary. Scale bar: 10 μ m.

Supplementary Figure 3

Filopodia merging occurred during PKC activation. Left panel shows a whole growth cone injected with Alexa 594 phalloidin at 2 min after PDBu addition. Right panel shows time montage of a region in the periphery (blue box). Colored arrow heads mark individual filopodia. Images were acquired every 10 sec with 10 min elapsed recording time.

Supplementary Figure 4

Actin network dynamics during PKC activation with or without myosin II activity.

(A) Actin flow vector maps from a growth cone injected with Alexa 594 phalloidin before and after PDBu (100 nM, 10 min) treatment. FSM images and flow speed maps of this growth cone are shown in Fig. 2A. (B) Another example of actin network dynamics during PKC activation. Actin FSM images (top) and corresponding flow vector maps (bottom) of a growth cone injected with Alexa 568 G-actin before and at different times after PDBu (100 nM) addition. P: peripheral domain; T: transition zone; C: central domain; red arrowhead: filopodium; yellow open arrowhead: actin arc; yellow arrow: intrapodia; red dotted circle: contractile node; red arrows mark a spot of veil retraction. (C) Actin flow vector maps from a growth cone injected with Alexa 594 phalloidin under control conditions, in blebbistatin (60 μ M, 10 min), and after PDBu (100 nM, 10 min) addition in blebbistatin background. FSM images and flow speed maps of this growth cones are shown in Fig. 4A. (D) Summary of changes in actin network translocation rates in P-domain, T-zone, and contractile node region before and after blebbistatin (60 μ M, 10-30 min) treatment. Data were normalized to those before blebbistatin addition.

(E-F) Average filopodium length (E) and growth cone spread (F) before and after treatment with blebbistatin. * $p < 0.01$ with two-tailed paired t-test. Number in parenthesis: growth cones measured. Scale bars: 5 μm .

Supplementary Figure 5

PKC activation did not increase baseline Ca^{2+} concentration in growth cones.

(A) Representative Ca^{2+} ratio images (top) and actin FSM with Alexa 594 phalloidin (bottom) of a growth cone before and after PDBu (100 nM, 5, 10, and 30 min) treatment. Ca^{2+} ratio encoded by a linear pseudocolor lookup table (see color bar). Images acquired every 10 sec for 13 min from -3 min before PDBu addition to 10 min after PDBu addition, then for 3 min at 30 min in PDBu. Scale bar: 10 μm . (B) Growth cone relative Ca^{2+} concentration (red line) and P-domain flow rates (green line) in response to PDBu over time. F_0 : average Ca^{2+} level immediately before PDBu addition. $F_t = \text{Ca}^{2+}$ level at a given time point. (C) Comparison of Ca^{2+} levels and P-domain flow rates before and after PDBu (100 nM, 20-30 min). The Ca^{2+} ratio imaging and FSM were carried out simultaneously. Images acquired every 10 s with 3-min elapsed recording time. Average Ca^{2+} levels and P-domain retrograde flow rates were normalized to those before PDBu addition (percentage of control), respectively. Values are expressed as mean \pm SEM. Statistical analysis was done by two-tailed paired t test. N = 6 growth cones. * $p < 0.001$ vs. before PDBu addition.

Supplementary Figure 6

PKC effects on actin network dynamics were independent of Rho kinase.

(A) Actin network visualized with phalloidin after fixation. Growth cones were treated with Y27632 (10 μ M, 20 min) or co-treated with Y27632 and PDBu (100 nM, 10 min) following Y27632 pretreatment (20 min). (B) Representative actin FSM images (top) and corresponding flow maps (bottom) from a growth cone injected with Alexa 594 phalloidin under control conditions (left), in Y27632 (10 μ M, 20 min), and after PDBu (100 nM, 10 min) addition in Y27632 background. Yellow dotted circle outlines the C-domain. (C and D) Summary of relative changes in P-domain, T-zone, and contractile node retrograde flow rates in response to Y27632 (10 μ M, 20-45 min, C), and to PDBu (100 nM, 10-30 min) in Y27632 background (D). Numbers in parentheses: growth cones measured. * $p < 0.01$ with two-tailed paired t-test. Scale bars: 10 μ m.

Supplementary Figure 7

Effects of PKC activation on PICK1 localization. Representative examples of actin filament (left column) and PICK1 immuno-localization (right column) under control conditions and after PKC activation for various times with 100 nM PDBu. Scale bars: 10 μ m.

Supplementary Figure 8

Aplysia myosin II regulatory light chain (RLC) cloning and characterization.

Aplysia nonmuscle myosin II regulatory light chain. (a) Schematic of conventional myosin II with regulatory light chains (green). (b) The predicted amino acid sequence of *Aplysia* neuronal myosin II RLC. Conserved RLC phosphorylation site (serine-16,

asterisk). (c) *Aplysia* RLC was bacterially expressed, purified, runs at ~19 kDa on SDS-PAGE, and used as antigen for polyclonal antibody production.

Movie Legends

These are AVI format movie files (.avi extensions). View using Windows Media Player.

Movie 1

PKC activation increased retrograde actin flow rates in growth cones.

FSM time lapse of F-actin dynamics in a growth cone injected with Alexa 594 phalloidin before and after 10 min in 100 nM PDBu. Scale bar: 5 μ m; 5 sec interval; elapsed time: 2 min; playback: 8 frames per sec. This movie is from the growth cone in Figure 2A.

Movie 2

Changes in actin dynamics during PKC activation.

FSM time lapse of F-actin dynamics in a growth cone injected with Alexa 568 G-actin before and immediately after addition of 100 nM PDBu (at frame 47). Scale bar: 5 μ m; 5 sec interval; elapsed time: 15 min; playback: 8 frames per sec. Note the slight focus shifts between frames 47-53 due to introduction of the drug. This movie is from the growth cone in Figure S4B.

Movie 3

Filopodia merging during PKC activation.

FSM time lapse of P domain F-actin dynamics in a growth cone injected with Alexa 594 phalloidin during 100 nM PDBu treatment. PDBu was added immediately before start of

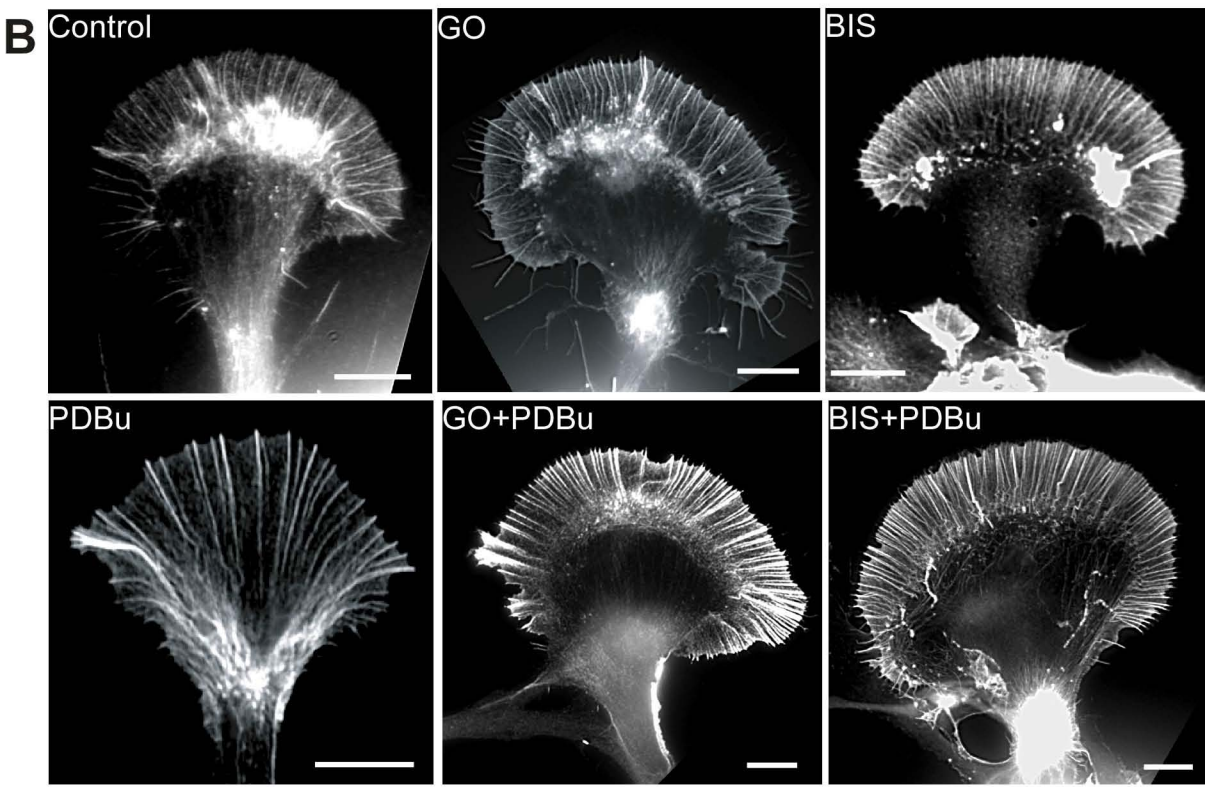
the movie. Scale bar: 5 μm ; 10 sec interval; elapsed time: 5 min; playback: 8 frames per sec. This movie is from the growth cone in Figure S3.

Movie 4

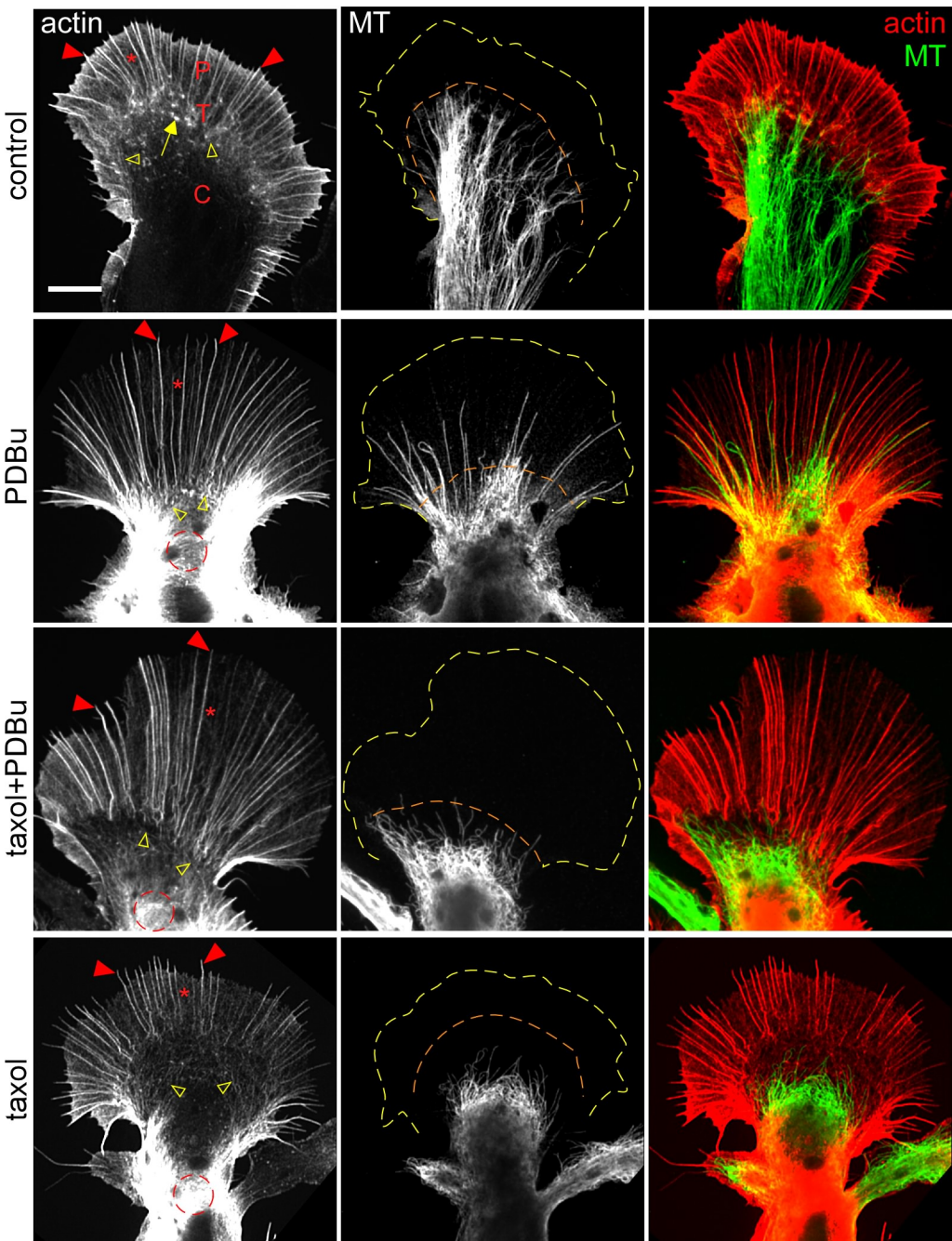
PKC activation did not increase retrograde flow in background of blebbistatin.

FSM time lapse of F-actin dynamics in a growth cone injected with Alexa 594 phalloidin under control conditions, in blebbistatin (60 μM , 10 min), and after PDBu (100 nM, 10 min) addition in blebbistatin background. Scale bar: 5 μm ; 5 sec interval; elapsed time: 2 min; playback: 8 frames per sec. This movie is from the growth cone in Figure 4A.

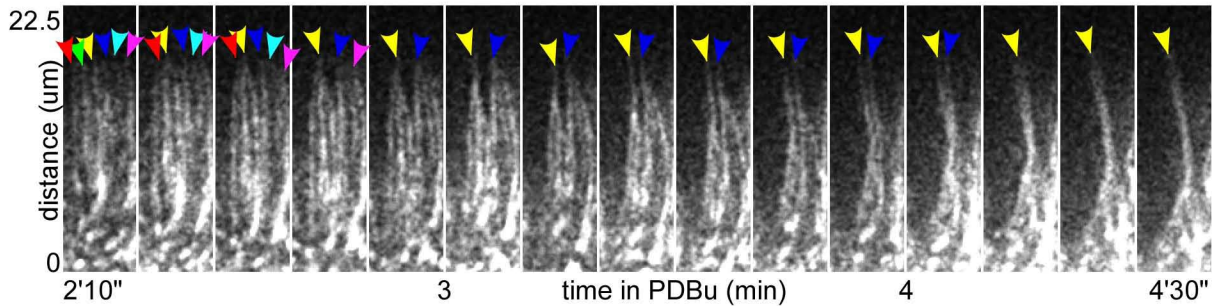
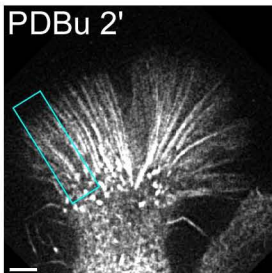
Supplementary Figure 1

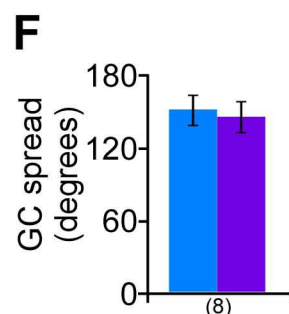
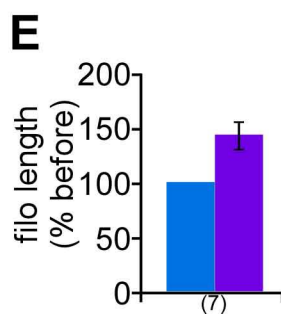
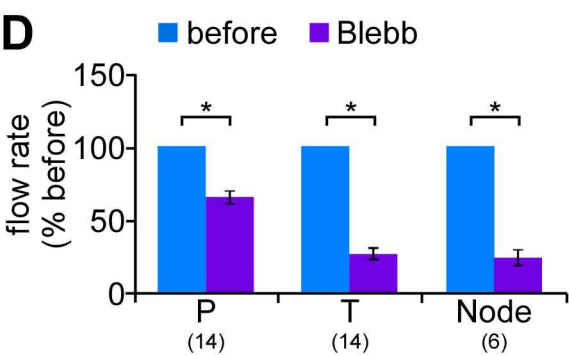
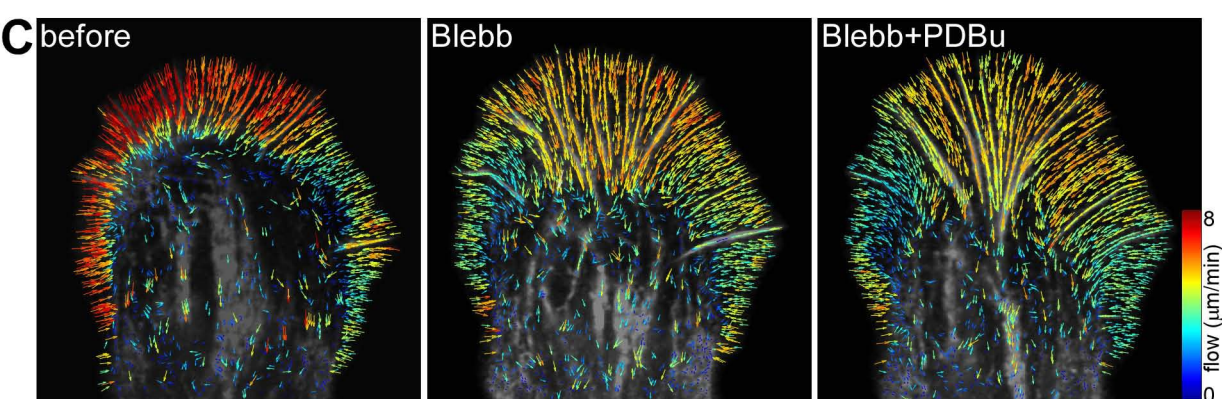
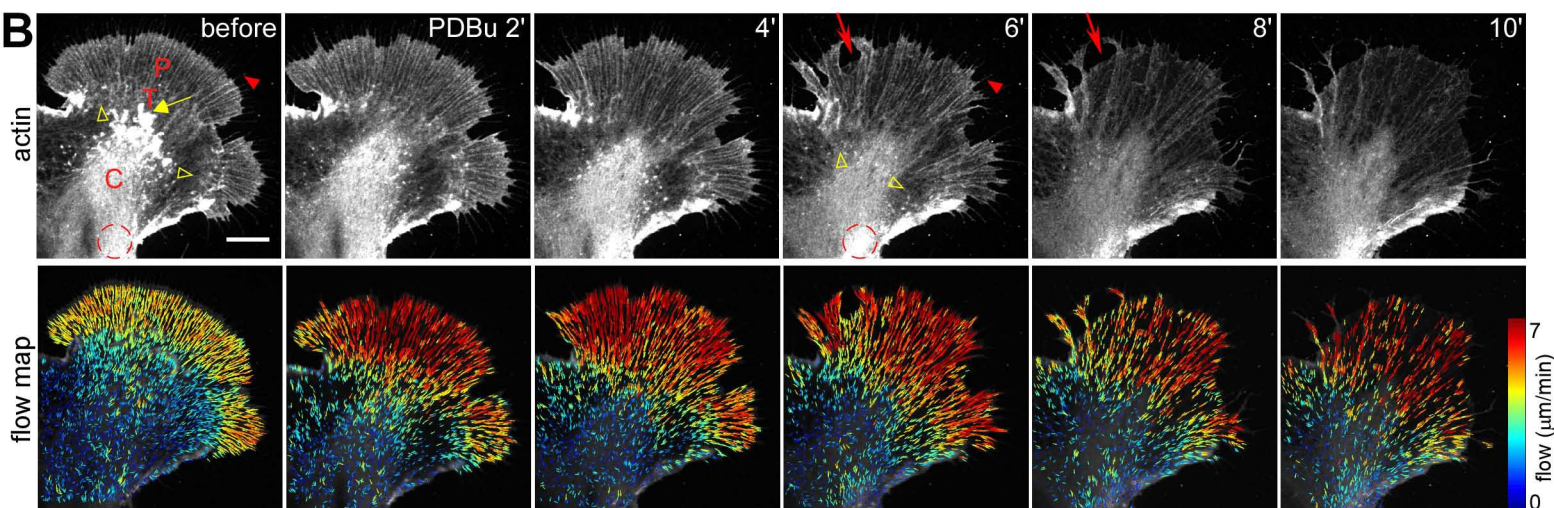
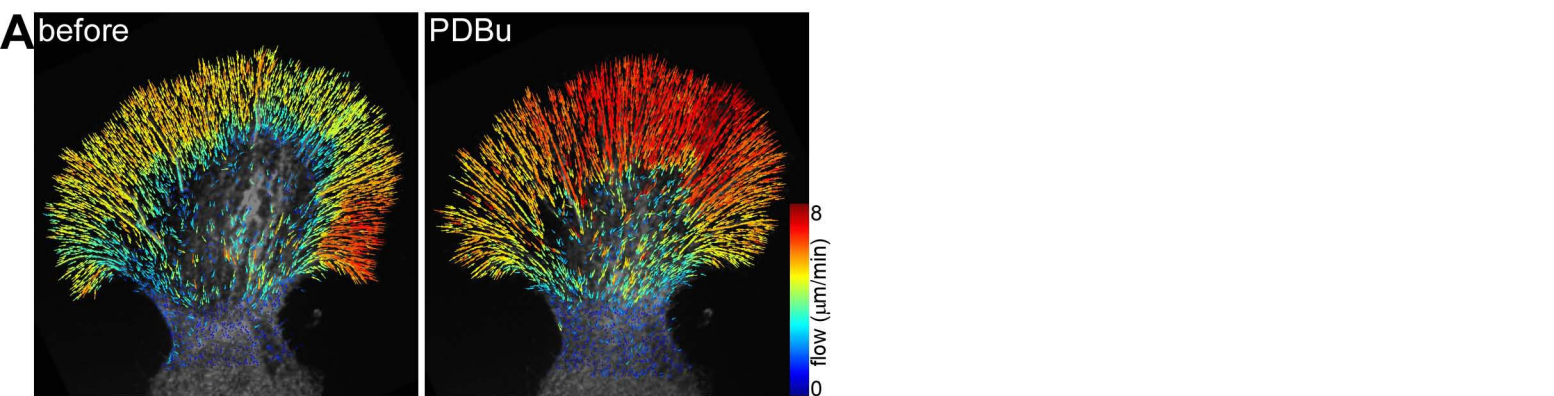


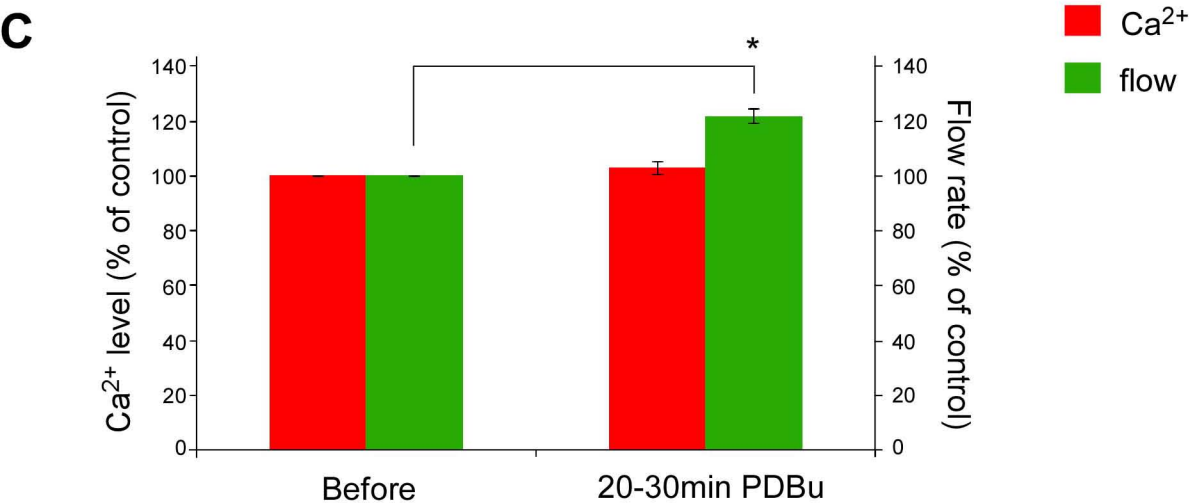
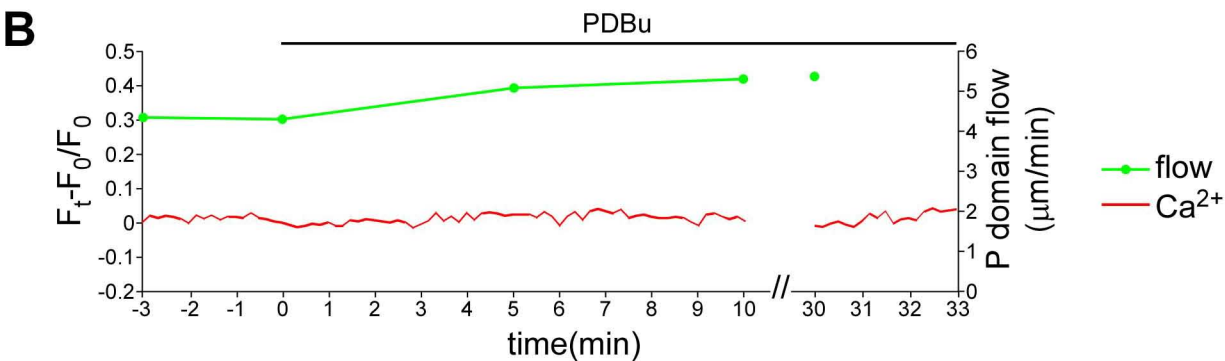
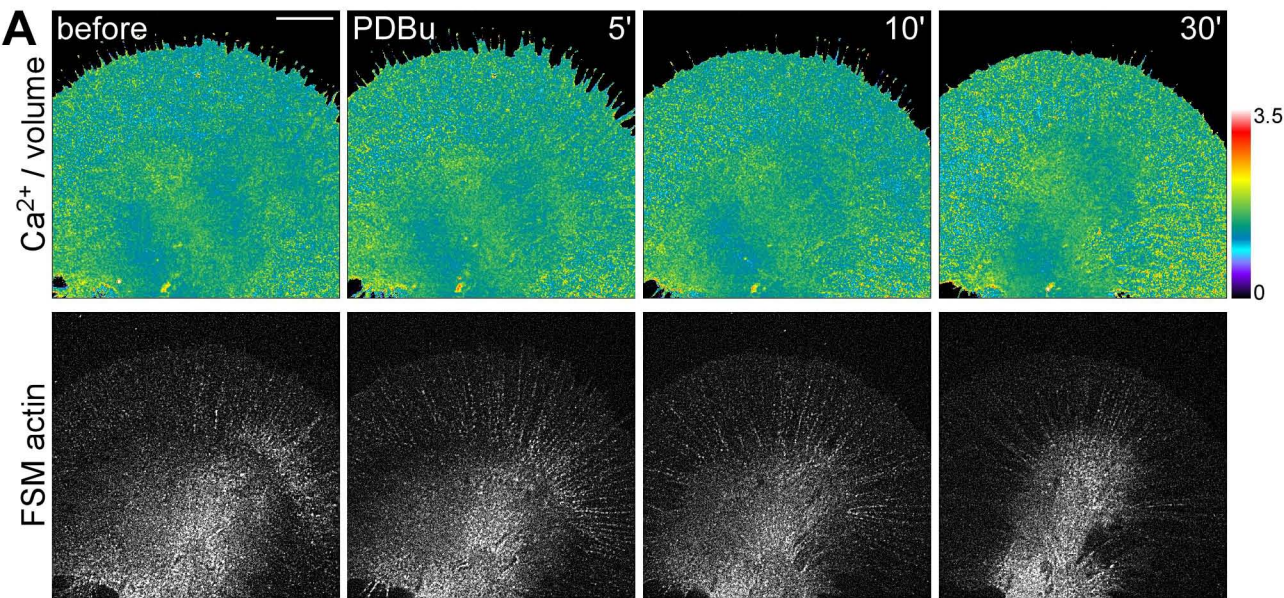
Supplementary Figure 2

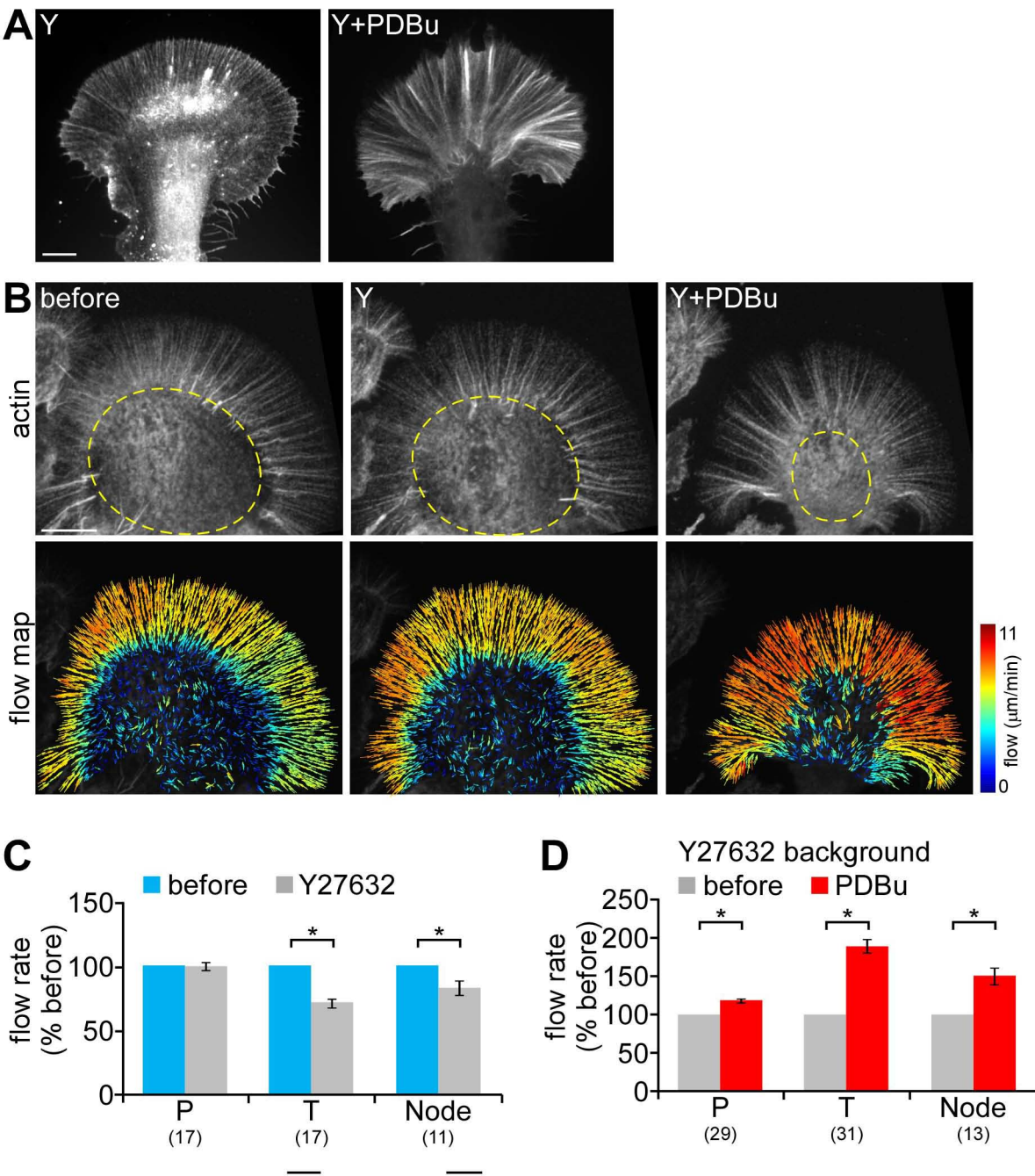


Supplementary Figure 3



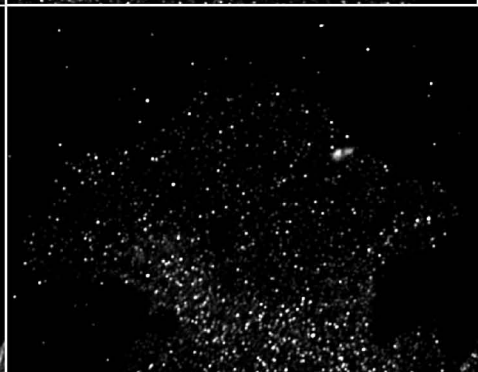
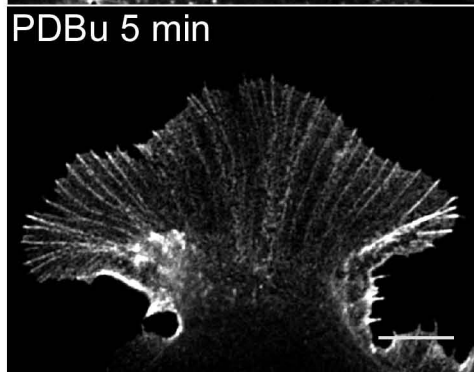
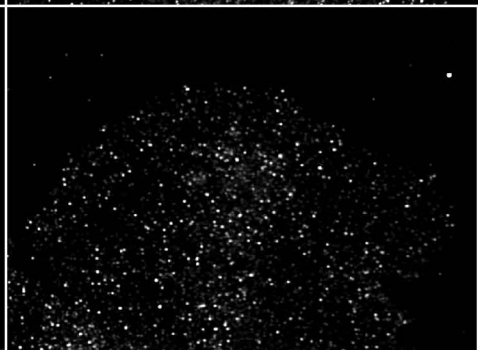
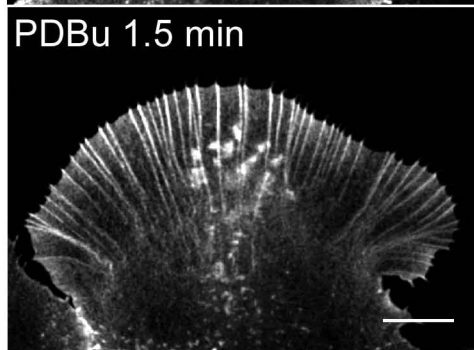
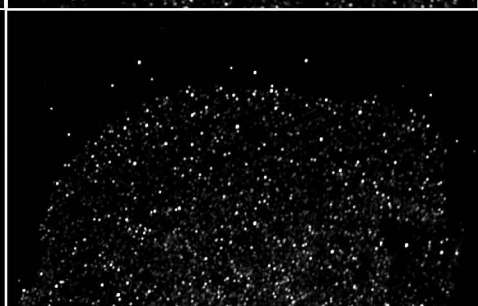
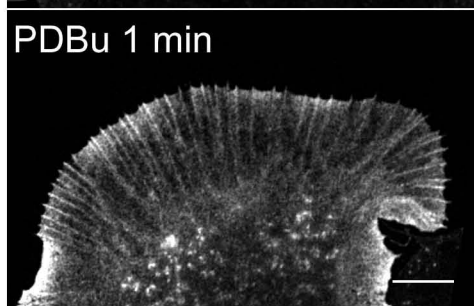
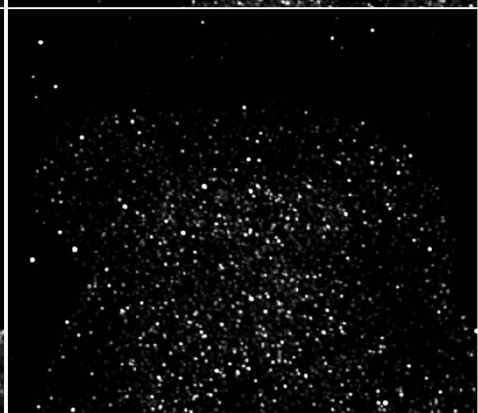
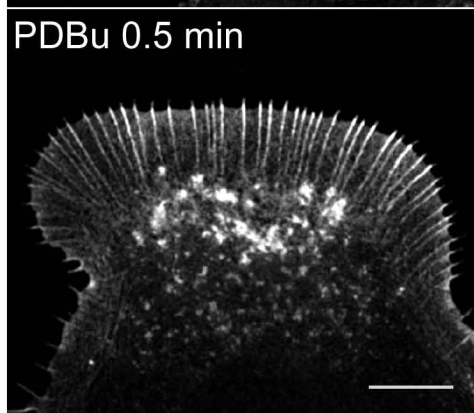
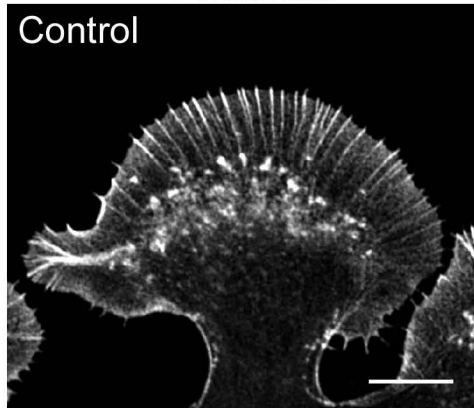






Phalloidin

PICK1



a



b

*

MAEEEDKKGR SGRATSNVFA KLSKKTMQEM KEAFTM DQN RDGI I DI EDL 50
 KDMYSNLGRI PPDAELNEML KEAPGPLNFT MFLNLFGEKL SGTDPEDTI R 100
 QAFSMFDGDG KGYI PEEYLK DLLSNMGDNF TAE EI KQTWK EAPLEKGFDF 150
 YGTFVGI LKG KEDEGES 167

c

